The MYC antagonist MNT autoregulates its expression and supports proliferation in MAX deficient cells.

M Carmen Lafita-Navarro[1,4], Judit Liaño-Pons[1], Andrea Quintanilla[1,5], Ignacio Varela[1], Fabiana Ourique[1,6], Gabriel Bretones[1,7], Rosa Blanco[1], Julia Aresti[1], Patrick Carroll[2], Peter Hurlin[3], Robert N. Eisenman[2], M. Dolores Delgado[1] and Javier León[1*]

[1]Instituto de Biomedicina y Biotecnología de Cantabria (IBBTEC), Universidad de Cantabria-CSIC, and Department of Molecular Biology, Universidad de Cantabria, Santander, Spain

[2]Division of Basic Sciences, Fred Hutchinson Cancer Research Center, Seattle, USA.

[3]Shriners Hospitals for Children Research Center, and Department of Cell, Developmental and Cancer Biology, Knight Cancer Institute, Oregon Health and Science University, Portland, USA.

[4]Present address: Sorrell lab, Department of Cell Biology UT Southwestern Medical Center, Dallas, USA

[5]Present address: Edinburgh Cancer Research UK Centre, Institute of Genetics and Molecular Medicine, University of Edinburgh, United Kingdom

[6]Present address: Department of Biochemistry, Universidade Federal de Santa Catarina (UFSC), Florianópolis, Brazil

[7]Present address: Departamento de Bioquímica y Biología Molecular, Facultad de Medicina, Instituto Universitario de Oncología (IUOPA), Universidad de Oviedo, Spain

*Corresponding author

Running title: MNT functions in the absence of MAX

Key words: MNT, MAX, MYC, MLX, transcription, promoter

ABSTRACT

MNT is a transcription factor of the MXD family. MNT-MAX dimers down-regulate genes by binding to E-boxes sequences, which can also be bound by MYC-MAX to activate transcription. MNT has been described as a modulator of MYC activity but little is known about MNT regulation and whether MNT has MAX-independent functions. Using a MAX deficient cell line and siRNA-mediated silencing of MAX, we show that in the absence of MAX the total MNT levels are elevated and that MNT localizes both in the cytoplasm and the nucleus. In contrast, MNT is predominantly nuclear when MAX is expressed. MNT is required for optimal cell proliferation even in the absence of MAX, being the first report of a MAX-independent function of MNT. Interestingly, MNT forms homodimers and autoregulates its expression by repressing its own promoter. The tight MNT regulation and its activity in absence of MAX suggest its importance on cell homeostasis.

INTRODUCTION

MNT (also called MXD6) is a basic helix-loop-helix leucine zipper (bHLHLZ) protein and it is the most divergent member of the MXD family, that also includes MXD1, MXI1, MXD3 and MXD4. MNT forms heterodimers with MAX through the bHLHLZ domain, and binds to E-box DNA sequences. MYC is one of the most prevalent human oncoproteins. MYC can also interact with MAX and bind E-boxes *(Conacci-Sorrell et al 2014, Dang 2012)*. Whereas MYC-MAX, upon binding to E-boxes, acts primarily as transcriptional activator, the typical effect of MNT-MAX is the transcriptional repression *(Hurlin et al 1997, Meroni et al 1997)*. MNT can bind not only to MAX but also to the MAX-like HLH protein MLX *(Billin et al 1999, Meroni et al 2000)* which alternatively can interact with MLXIP (MONDOA) and MLXIPL (MONDOB) proteins. Therefore, MNT participates both in the MAX- and MLX-centred networks [reviewed in *(Diolaiti et al 2015, Yang & Hurlin 2017)*] serving as the link between the MAX-MYC and MLX-MONDO networks.

MNT is expressed constitutively in proliferating and quiescent cells and protein levels do not show major fluctuations when quiescent cells are mitotically stimulated *(Hurlin et al 1997 , Hurlin et al 2003, Walker et al 2005)* . MNT$^{-/-}$ mice are not viable *(Hurlin et al 2003, Toyo-oka et al 2004)* while MXD1$^{-/-}$, MXI1$^{-/-}$ and MXD3$^{-/-}$ mice survive, suggesting that MNT function is not redundant with that of the other MXD proteins *(Foley et al 1998, Queva et al 1999, Schreiber-Agus & DePinho 1998)*. Moreover, MNT is the only MXD protein in invertebrates *(Diolaiti et al 2015)*.

Consistent with MNT functioning as a MYC transcriptional antagonist, enforced MNT expression inhibits cell proliferation and impairs MYC-dependent transformation

63 *(Hurlin et al 1997, Walker et al 2005)*. The deficiency or down-regulation of MNT in
64 fibroblasts leads to increased proliferation (i.e., similarly to MYC-overexpression) and
65 partially rescues the proliferative arrest caused by MYC ablation *(Dezfouli et al 2006,*
66 *Hurlin et al 2003, Nilsson et al 2004, Walker et al 2005)*. MNT ablation *in vivo* leads to
67 breast and T-cell tumors *(Dezfouli et al 2006, Hurlin et al 2003, Toyo-oka et al 2004)*. On
68 the other hand, MNT knock-out in some cell models inhibits proliferation, promotes
69 apoptosis *(Dezfouli et al 2006, Hurlin et al 2003, Nilsson et al 2004)* and impairs MYC-
70 dependent tumorigenesis *(Link et al 2012)*. Thus, as MYC and MNT coexist in
71 proliferating cells, it has been suggested a role of MNT as a "buffer" of MYC activity.
72 We took advantage of a cell line deficient in MAX to explore possible MAX-
73 independent functions of MNT. UR61 cells, derived rat pheochromocytoma, do not
74 express a functional MAX protein but a truncated form (termed MAX^{PC12}) encoding a that
75 lacks the second helix and leucine zipper region of the bHLH-LZ domain which are the
76 regions responsible for dimerization with MYC and MNT *(Hopewell & Ziff 1995)*. Here
77 we describe that, in UR61 cells, MNT localizes both in the cytoplasm and in the nucleus,
78 but it is exclusively nuclear when MAX is re-expressed. Moreover, MNT autoregulates
79 its expression through binding and transrepressing its own promoter in the presence of
80 MAX. MNT was required for optimal cell proliferation even in the absence of MAX, being
81 the first example of MAX-independent function of MNT. Furthermore, RNA-seq
82 experiments showed that MNT can regulate gene expression in the absence of MAX.
83
84

85 **RESULTS**

86 **MNT levels depend on MAX**

87 We first studied MNT levels in proliferating cells from eleven cell lines derived from
88 different tissues and species, including two cell lines lacking MAX: UR61 and human
89 small cell lung carcinoma H1417 cells *(Romero et al 2014)*. The results showed that,
90 although MNT expression varies among cell lines, the two MAX-deficient cell lines
91 expressed high MNT levels (*Figure 1A*). MNT was expressed in all cell lines as a protein
92 doublet, due to a slower migrating phosphorylated MNT form *(Popov et al 2005)*.
93 The high MNT expression in the two MAX-deficient cell lines led us to explore
94 whether MAX influenced MNT levels. For this purpose, we transfected UR61 cells with
95 a construct carrying human MAX cDNA driven by the metallothionein promoter, which is
96 activated by Zn^{2+} cations *(Canelles et al 1997)*. Several clones were isolated and two of
97 them with robust MAX induction were mixed and the resulting cell line was termed

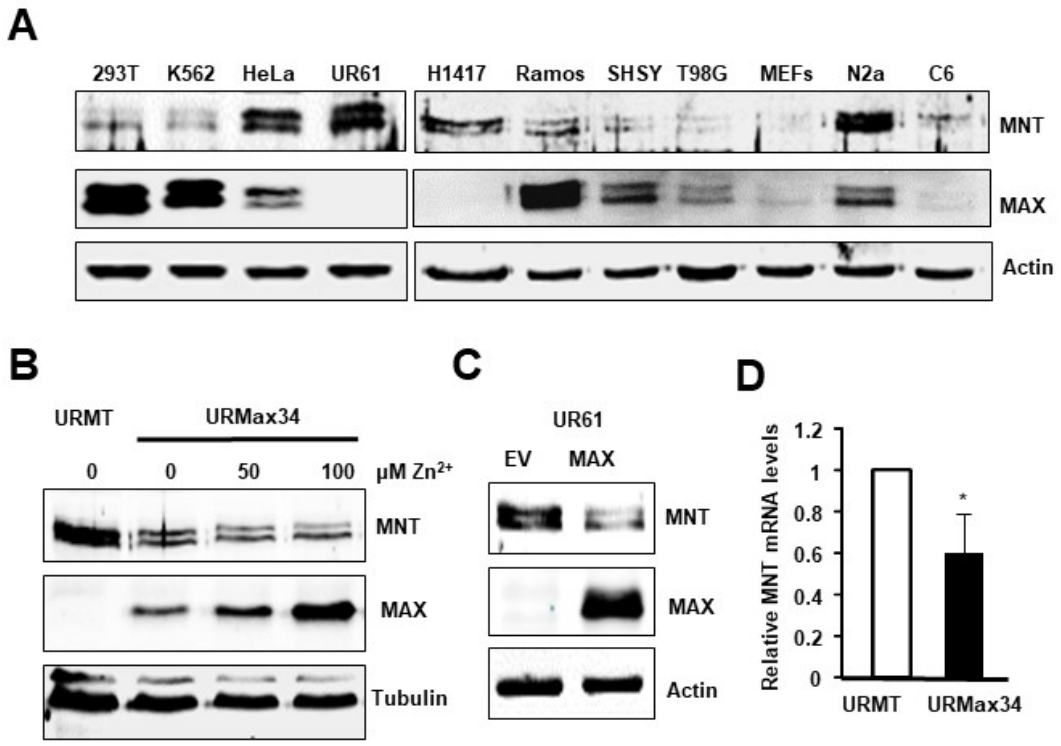

Figure 1. High MNT expression in MAX-deficient cells. (A) Cell lysates of the indicated cell lines were analyzed by immunoblot to determine the levels of MNT and MAX. β-actin levels were determined for protein loading control. The MAX-deficient cell lines analyzed were: UR61 (rat pheochromocytoma) and H1417 (human small cell lung carcinoma). The rest are MAX-expressing cells: HEK293T (human embryonic kidney, 293T), K562 (human chronic myeloid leukaemia), HeLa (human cervical cancer), Ramos (human B cell lymphoma), SH-SY-Y5 (SHSY, human neuroblastoma), T98G (human glioblastoma), MEFs (mouse embryonic fibroblasts), Neuro-2a (N2a, mouse neuroblastoma) and C6 (rat glioma). (B) Control URMT and URMax34 cells were treated for 24 h with 50 and 100 μM Zn^{+2} and the MNT and MAX protein expression were determined by immunoblot. α-tubulin levels were determined as a control for protein loading. (C) Levels of MNT and MAX determined by immunoblot in UR61 cells 24 h after transfection with a MAX expression vector or the empty vector pCEFL (EV). β-actin levels were determined as a control for protein loading . (D) mRNA expression determined by RT-qPCR in URMT and URMax34 cells treated for 24 h with 100 μM Zn^{2+}. Data are represented as mean ±s.d. from three independent experiments, *P<0.01

URMax34. We also generated a cell line transfected with the empty vector, termed URMT. The induction of MAX in response to Zn^{2+} in URMax34 cells was confirmed by immunoblot (*Figure 1B*). We examined the effect of MAX induction on MNT levels in URMax34 cells. The results showed that MNT was down-regulated upon MAX induction by Zn^{2+} (*Figure 1B*). To confirm this result and rule out effects potentially related to the generation of stably transfected clones (as URMax34 system), UR61 cells were transiently transfected with a MAX expression vector and the results showed a decrease in MNT protein levels in MAX-transfected cells (*Figure 1C*). It is noteworthy that the r-expression of MAX in these cells provoked the down-regulation of MNT at the mRNA levels, as determined by RT-qPCR (*Figure 1D*).

We sought to confirm this in a different cell type and species. For this purpose a MAX expression vector was transfected into human myeloid leukemia K562 cells. The immunoblot results showed lower MNT levels in the cells with MAX overexpression

111 (*Figure 2A*). Next, we used the Kmax12 cell line *(Canelles et al 1997)*, a K562 derivative
112 carrying a MAX transgene which expression is induced by Zn^{2+}. Induction of MAX
113 expression in Kmax12 cells resulted in a concomitant MNT downregulation (*Figure 2B*).
114 We also used the opposite approach, i.e. depleting cells of MAX and analyzing the
115 expression of MNT. As shown in *Figure 2C*, MNT protein expression was upregulated
116 when MAX was silenced with siRNA in K562. Interestingly, MNT mRNA was also up-
117 regulated in MAX-silenced cells (*Figure 2D*). Altogether, the results showed that low MAX
118 levels result in MNT up-regulation, likely at the transcriptional level.

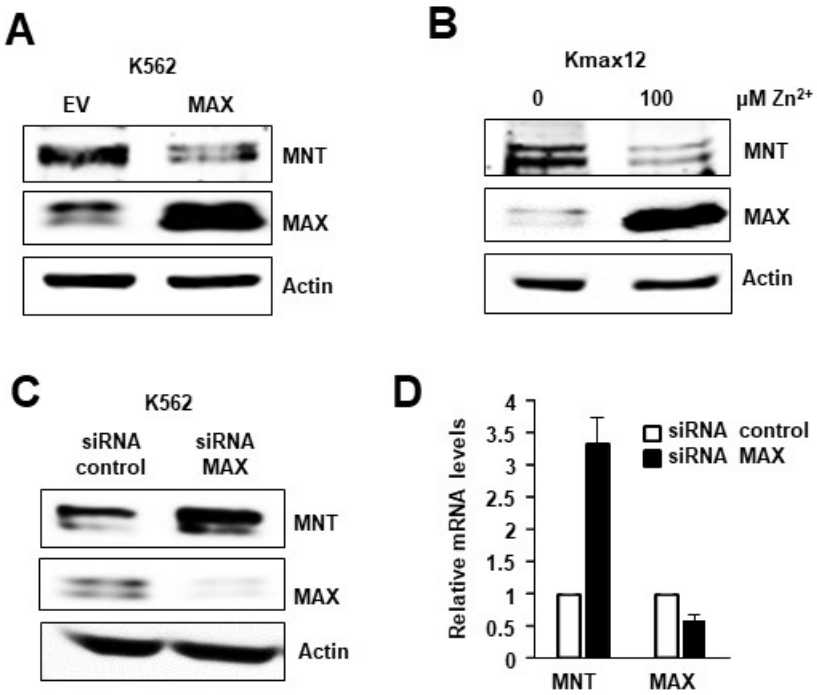

Figure 2. MAX regulates MNT expression in K562 cells. (A) MNT and MAX levels determined by immunoblot in K562 cells 24 h after transfection with a MAX expression vector. (B) MNT and MAX levels determined by immunoblot in Kmax12 cells treated for 48 h with 100 μM Zn^{2+} to induce MAX expression. (C) MNT and MAX protein expression analyzed by immunoblot in K562 48 h after transfection with siRNA against *MAX* gene. β-actin levels are shown as a protein loading control. (D) MNT and MAX mRNA expression analyzed by RT-qPCR 48 h after transfection with siRNA against *MAX* gene. Data are shown as mean ± s.d. from three independent experiments.

119

120 **MNT binds and repress its own promoter in the presence of MAX**

121 The above results showing that MNT down-regulation took place at the mRNA
122 level prompted us to investigate if MNT impairs the activity of its own promoter.
123 Bioinformatic analysis of human, mouse and rat MNT promoter regions revealed that
124 there are two E-box sequences within 1 kb upstream the transcriptional start site of *MNT*
125 (one canonical Ebox, CACGTG, and one non-canonical, CATGTG) that are conserved
126 among these three different species (Figure 3A).

127 We then constructed a luciferase reporter carrying the 850 bp upstream region
128 of the transcription start site from the human MNT gene. The construct was termed
129 850MNT-Luc (Figure 3B). HEK293T cells (which express MAX) were transfected with
130 the 850MNT-Luc and MNT expression vectors. The results showed that MNT
131 overexpression led to a reduction in the luciferase activity (Figure 3C), suggesting that
132 MNT-MAX negatively regulates the MNT promoter. To determine the contribution of the

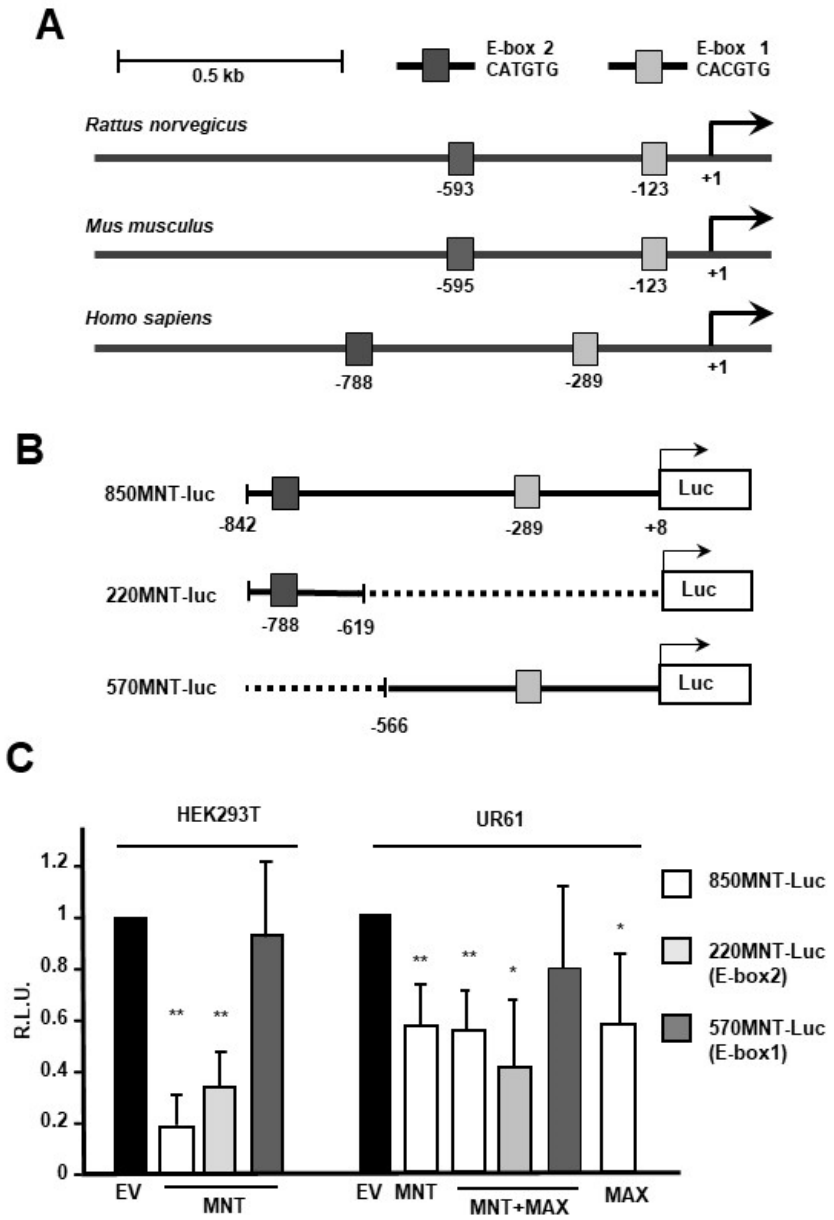

Figure 3. MNT regulates its own promoter. (A) Schematic representation of human, rat and mouse MNT promoters showing two conserved E-boxes. The coordinates correspond to the 5' nucleotide of each E-box, using the UCSC genome browser (http://genome.ucsc.edu/, release GRCh37/hg19). (B) Schematic representation of luciferase reporters driven by human MNT promoter generated in this work. The longest reporter (850 bp upstream the transcription start site) contains two conserved E-boxes. The coordinates are as in USCS browser (release GRCh37/hg19). (C) Luciferase assays in the indicated cell lines transfected with the reporters described above plus MNT and/or MAX expressing vectors or the corresponding empty vectors (EV). Luciferase activity was assayed 36 h or 24 h after transfection of UR61 and HEK293T cells, respectively. The data are shown as mean ± s.e.m. of 9 (for 850MNT-luc) or 4 independent transfections (for the rest of experimental points). $^{**}P < 0.005$; $^{*}P < 0.01$.

133 two E-boxes in the MNT-mediated autoregulation we constructed two reporters
134 containing each of the E-boxes, termed 220MNT-Luc (containing 220 bp of the promoter
135 including E-box 2) and 570MNT-Luc (containing 570 bp of the promoter, including E-box
136 1 (Figure 3B). The luciferase assays in HEK293T cells showed that the E-box 2, mapping
137 at –788 was critical for MNT-mediated downregulation of its own promoter (*Figure 3C*,
138 left panel).

139 We also investigated the activity of the MNT promoter in UR61 cells, which do
140 not express MAX. UR61 cells were transfected with the 850MNT-Luc vector together
141 with MNT and MAX expression vectors. The results also showed a decrease in the
142 luciferase activity although less than in HEK293T cells (*Figure 3C*, right panel). The
143 expression of MNT alone also led to a decrease in the luciferase activity, suggesting that
144 MNT can downregulate MNT promoter in UR61 cells in the absence of MAX. The
145 repressive effect of MNT was stronger in HEK293T cells than in UR61 cells, which may
146 be explained by the limited overexpression of MNT protein achieved in transfected UR61
147 cells (see below). Co-transfection of MNT and MAX resulted in a decrease in the activity
148 of both promoter constructs (850MNT-
149 Luc and 220MNT-Luc, carrying
150 fragments of the human MNT
151 promoter of 842 and 223 bp,
152 respectively). Since MNT-MAX dimers
153 bind E-boxes in the promoters to
154 repress transcription, we analysed the
155 ChIP-seq data published by the
156 ENCODE project
157 (http://genome.ucsc.edu/ENCODE).
158 The data revealed two regions bound
159 by MAX in the human *MNT* promoter
160 that encompass the two E-boxes
161 (*Figure 4A*). We also analysed the
162 ChIP peaks for MAX, MYC and MXI1
163 proteins on the *MNT* promoter in other
164 human cell lines as H1ES, HeLa,
165 NB4, A549, GM78, HEPG, SKSM and
166 IMR90. The analysis revealed that the
167 three proteins presented peaks at the
168 same positions near the transcription

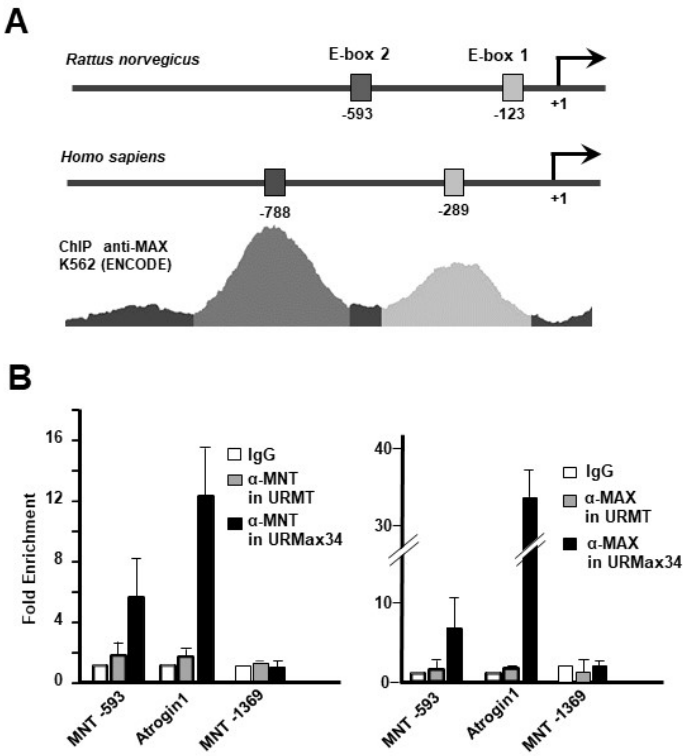

Figure 4. MNT binds to *MNT* promoter. (A) Schematic representation of human and rat MNT promoters showing and the peaks of MAX of the ChIP experiments with anti-MAX antibody on human K562 cell line as published by the ENCODE project. (B) ChIP with anti-MNT (left) and anti-MAX (right) antibodies on the MNT promoter of URMT and URMax34 cells, both treated with 100 μM Zn^{2+} for 24 h. MNT and MAX binding to *MNT* gene promoter in the region containing the E-box 2 (-593 in rat gene) was studied by qPCR. Amplicons from Atrogin-1 (*FBX032*) were used as positive control for MNT binding and a region 1389 bp upstream from the TSS without E-boxes was used as negative control. The data are represented as mean ±s.e.m. from four independent experiments.

169 start site of the human MNT gene (*Supplementary Figure 1*), suggesting that members
170 of the MYC and MXD family bind and possibly regulate the promoter of *MNT*.
171 As MNT was downregulated when MAX was re-expressed, we hypothesized that
172 MNT-MAX heterodimers might bind to the *MNT* promoter and down-regulate its own
173 expression. To explore this hypothesis, a ChIP assay was performed with MNT and MAX
174 antibodies in URMT and URMax34 treated with Zn^{2+} to induce MAX. We studied the -
175 593 E-box of *MNT* promoter, as well as a region of the *Atrogin-1 (FBXO32)* promoter as
176 a positive control for MNT binding *(Terragni et al 2011)*. A region mapping at 1369 bp
177 upstream on MNT transcription start site with no E-boxes was used as negative control.
178 As shown in *Figure 4B*, MNT and MAX bound to the *MNT* promoter in URMax34 cells.
179 However, in the MAX-deficient control URMT cells, neither MNT nor MAX were bound to
180 *MNT* promoter. In the same way, MNT and MAX were bound to the positive control
181 *Atrogin-1* promoter in URMax34 but
182 not in URMT control cells (*Figure*
183 *4B*). These data show that MNT
184 binds to its own promoter as a
185 heterodimer with MAX and suggest
186 a possible negative regulation of its
187 own expression.
188
189 **MNT localizes in the**
190 **cytoplasm of MAX-deficient**
191 **cells**We next examined the
192 subcellular localization of the
193 excess MNT present in MAX-
194 deficient cells. URMT and
195 URMax34 cells were treated with
196 Zn^{2+} to induce MAX and we
197 performed a cytoplasmic and
198 nuclear fractionation to analyse
199 MNT levels. In control URMT cells,
200 MNT protein was found in the
201 nuclear fraction, as expected, but
202 also at similar levels in the
203 cytoplasm. In contrast, in URMax34
204 expressing MAX, MNT protein was

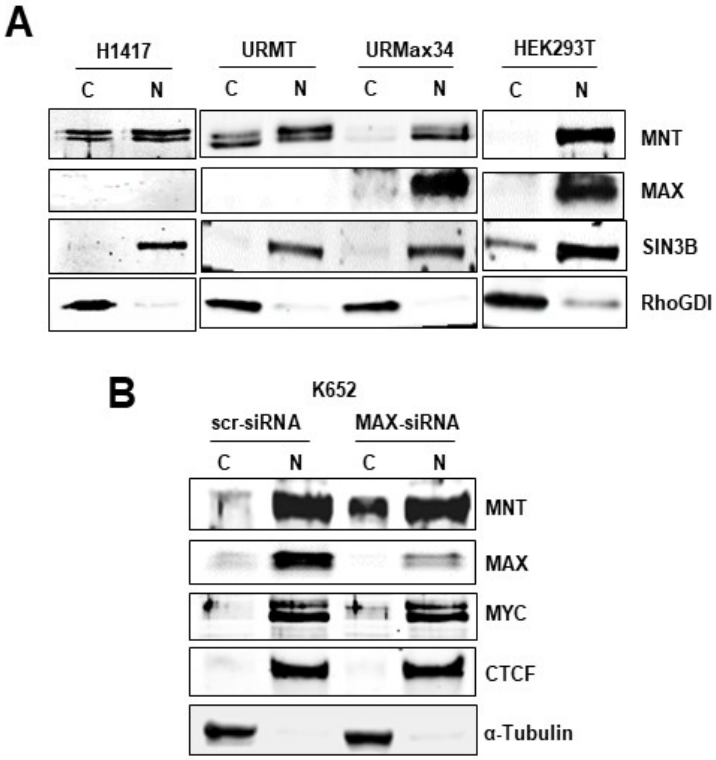

Figure 5. MNT subcellular localization depends on MAX. (A) Cell extracts were subjected to cytoplasmic/nuclear fractionation in H1417 (human lung cells deficient in MAX), HEK293T, URMT and URMax34 treated for 24 h with 100 μM Zn^{2+} to induce MAX. The levels of MNT and MAX were determined in each fraction by immunoblot. SIN3B and RhoGDI (ARHGDIA) were used as nuclear and cytoplasmic markers respectively. "C" refers to cytoplasmic fraction and "N" to nuclear fraction. (B) K562 were transfected with siRNA against the *MAX* gene and 48 h later cell extracts were prepared and subjected to cytoplasmic/nuclear fractionation. The expression of MAX, MNT and MYC were analyzed by immunoblot. The expression of CTCF and α-tubulin were analyzed as a control for nuclear and cytoplasmic proteins respectively. scrRNA, control scrambled siRNA.

205 found only in the nucleus (*Figure 5A*), the localization typically found for MNT *(Lafita-*
206 *Navarro et al 2016)*. We could not use untreated URMax34 cells as a control as they
207 express some MAX even in the absence of Zn^{2+} (*Figure 1B*). Cytoplasmic MNT was also
208 observed in H1417 cells, human cells deficient in MAX. As a control, the localization of
209 MNT was analysed in HEK293T cells, that express the MAX protein. Cytoplasm/nucleus
210 fractionation revealed that MNT and MAX were localised in the nucleus but not in the
211 cytoplasm of HEK293T cells (*Figure 5A*). To test if the localization of MNT depended on
212 MAX, we silenced the MAX protein in K562 cells with siRNA and we carried out
213 cytoplasm/nucleus fractionation. In control K562 cells, MNT and MAX were mainly
214 localised in the nucleus. In contrast, in MAX-depleted cells, a significant amount of MNT
215 was found in the cytoplasm of K562 cells (*Figure 5B*). It is noteworthy that nuclear MNT
216 levels were similar in URMT and URMax34, as well as in control K562 and MAX-depleted
217 K562 cells. As controls for nuclear proteins, we used MYC and CTCF (*Figure 5B*). Taken
218 together, the data indicates that MAX absence leads to an upregulation of MNT protein
219 and that the excess of MNT accumulates in the cytoplasm.
220

221 **MNT knock-down impairs cell proliferation in MAX-deficient cells**

222 We next asked for a possible biological effect of MNT on cell proliferation in the MAX-
223 deficient cells. Although we tried to generate UR61 sublines stably transfected with MNT,
224 we were not able to detect a significant increase in MNT protein levels upon transfection
225 of MNT expression vectors. This is likely due to the autoregulation of MNT protein levels,
226 as the overexpression of MNT protein was readily detected by immunoblot when the
227 transfected cells were treated with the proteasome inhibitor bortezomib (*Supplementary*
228 *Figure 2A*). In contrast, some increase in the the levels of MNT was detected when MNT
229 was transfected in MAX-expressing URMax34 cells (*Supplementary Figure 2B*) or when
230 MNT was co-transfected with MAX in UR61 cells (*Supplementary Figure 2C*).
231 Therefore, as significant MNT overexpression was not attainable in UR61 cells,
232 we decided to knock-down MNT through siRNAs. For this, we used lentiviral particles
233 containing two short-hairpin constructs against the rat MNT gene. Two shMNT constructs
234 that efficiently reduced MNT levels were used, termed shMNT-1 and shMNT-2 (*Figure*
235 *6A*). The vectors also carried a puromycin-resistance gene.UR61 cells were transiently
236 co-transfected with the shMNT constructs (or the empty vector) and a GFP expression
237 vector in a proportion 1:5 to ensure that the GFP-positive cells also incorporated the sh-
238 MNT plasmid. Six days after transfection, the fraction of GFP positive cells were
239 analysed by flow cytometry. The results showed that the fraction of GFP positive cells
240 was clearly reduced in cells with depleted MNT (*Figure 6B*), suggesting that MNT loss

241 resulted in impaired cell proliferation. In a second approach, we transfected the UR61
242 cells with the sh-MNT constructs and counted viable cells after 3 and 7 days of
243 transfection. As shown in *Figure 6C,* MNT-silenced UR61 cells grew slower than
244 controls. We also performed clonogenic assays in UR61 transfected with the shMNT
245 and/or a MAX expression vector (in 1:3 proportions to ensure that the
246 shMNT containing cells had also incorporated the MAX vector) as well as the empty
247 vectors. 24 h after transfection puromycin was added and after selection the colonies
248 were stained with crystal violet, the dye was solubilised and quantified. The results

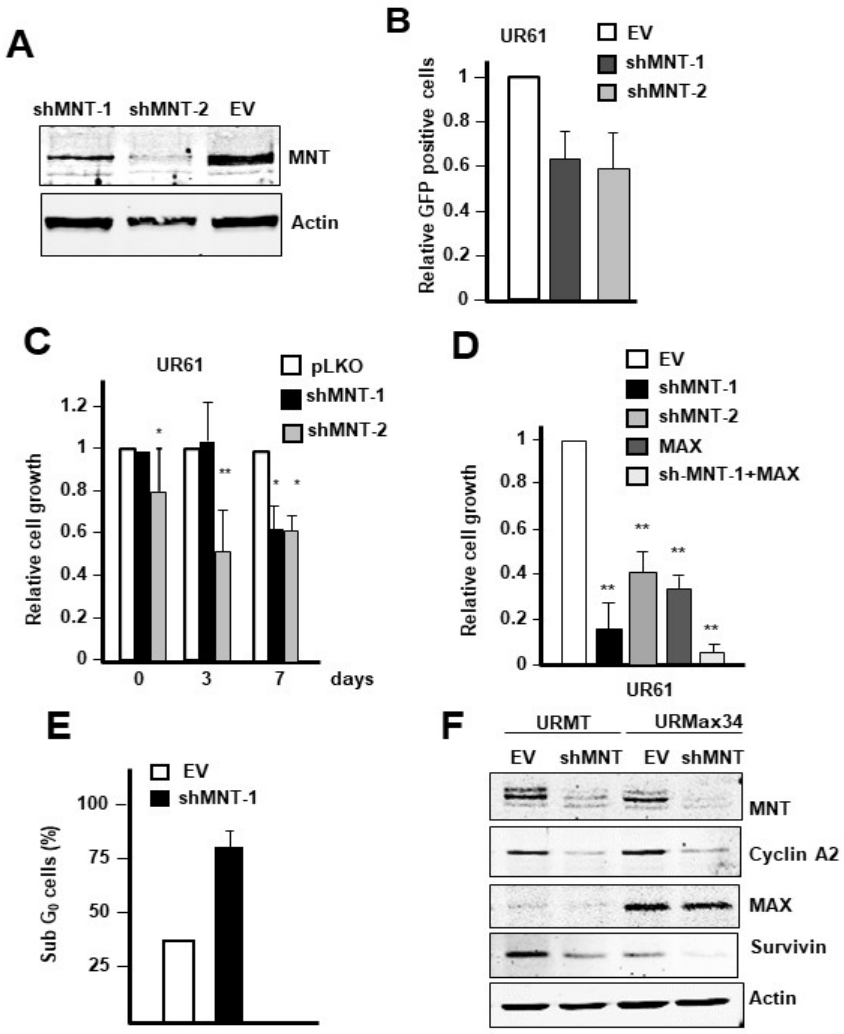

Figure 6. MNT knock-down impairs cell proliferation in MAX-deficient cells. (A) Silencing of MNT by shot-hairpin constructs. URMT cells were transfected with vectors encoding sh-MNT-1 and shMNT-2. 24 h after transfection the cells were treated with puromycin (0,5 µg/ml) and 72 h after transfection the cells were lysed and the levels of MNT analyzed by immunoblot. β-actin levels were determined as a control for protein loading. (B) Fraction of GFP-expressing UR61 cells assessed by flow cytometry 7 days after co-transfection with GFP and shMNT vectors (in proportion 1:5) and analyzed by flow cytometry. (C) Cell proliferation determined by cell counting at 3 and 7 days after transfection of shMNT vectors or empty vector. (D) Cell growth determined by crystal violet staining in UR61 cells transfected with the indicated vectors. After 15 days of puromycin selection the colonies were stained with crystal violet and the dye was solubilised and quantified. EV, empty vector (pLKO for shMNTs and pCEFL for MAX). **P < 0.005; *P <0.05. Data show mean values ± s.d. from at least three independent experiments. (E) Fraction of sub G_0 UR61 cells transfected with the shMNT-1 vector and empty vector (EV). Cells were fixed and stained with propidium iodide at day 6 post-transfection and puromycin selection. The percentage of cells containing less than 2C DNA content was determined by flow cytometry. The data are mean values of three independent experiments ± s.d. (F) Levels of MNT determined by immunoblot in URMT and URMax34 cells 72 h after transfection with the sh-MNT vector and treated for 12 h with 100 µM Zn^{2+}. MAX, cyclin A2, nd surviving (BIRC5) were also determined. β-actin levels were determined for protein loading control

249 showed that MNT depletion provoked a dramatic growth inhibition. The result that MNT
250 depletion impaired cellular proliferation in a MAX-independent manner is unprecedented.
251 The results also showed that UR61 cells overexpressing the MAX protein grew more
252 slowly than the control *(Figure 6D),* as reported for the MAX-deficient parental PC12
253 pheochromocytoma cells *(Hopewell & Ziff 1995)*. When MNT silencing was accompanied
254 by MAX enforced expression, the inhibition of UR61 cell proliferation was stronger
255 (*Figure 6D*). Consistent with the anti-proliferative effects of MNT depletion, we failed to
256 generate stably MNT-silenced UR61 (not shown).

257 Since MNT impairs cell proliferation of UR61 cells, we wondered whether this
258 was accompanied by cell death. To study this, the levels of survivin (BIRC5) in URMT
259 and URMax34 was analysed by immunoblot and the results showed a decrease in
260 survivin and cyclin A (a marker of proliferation) in cells with depleted MNT, both in MAX-
261 deficient cells (compare lanes 1 vs 2) and in MAX-expressing cells (compare lanes 3 vs
262 4), although the effect was stronger in these latter cells. To check the contribution of
263 apoptosis, we also measured DNA content flow cytometry. We found that the fraction of
264 cells with a sub-G0 amount of DNA was higher in cells transfected with the sh-MNT
265 vector (Figure 6F). The results suggest that the depletion of MNT leads to cell
266 proliferation arrest and apoptosis in UR61.

267

268 **MNT modifies gene expression in MAX-deficient cells**

269 Since the data shown above indicates that MNT knock-down in UR61 cells leads to
270 growth arrest, and considering that MNT is a transcription factor, we set out to study if
271 MNT alters the transcriptional program in the absence of MAX. For this purpose, we
272 investigated the effects of MNT depletion on the transcriptome of cells with and without
273 MAX. URMT and URMax34 cells were transfected with the short-hairpin RNA constructs
274 against the rat MNT gene (shMNT-1) or the empty vector as control. Two days after
275 transfection, when a significant depletion of MNT protein was observed (*Figure 7A*), cells
276 were treated with Zn^{2+} for 24 h to achieve MAX induction when appropriate. Then, lysates
277 to test MNT expression and total RNA were prepared. Two independent transfections
278 and RNA preparations of each cell line were analyzed. The upregulation of MAX in
279 response to Zn^{2+} in URMax34 cells and downregulation of MNT in cells transfected with
280 shMNT-1 was confirmed by immunoblot in the two duplicates (*Figure 7A*). The RNAs
281 were submitted for ultrasequencing and the RNA-seq.

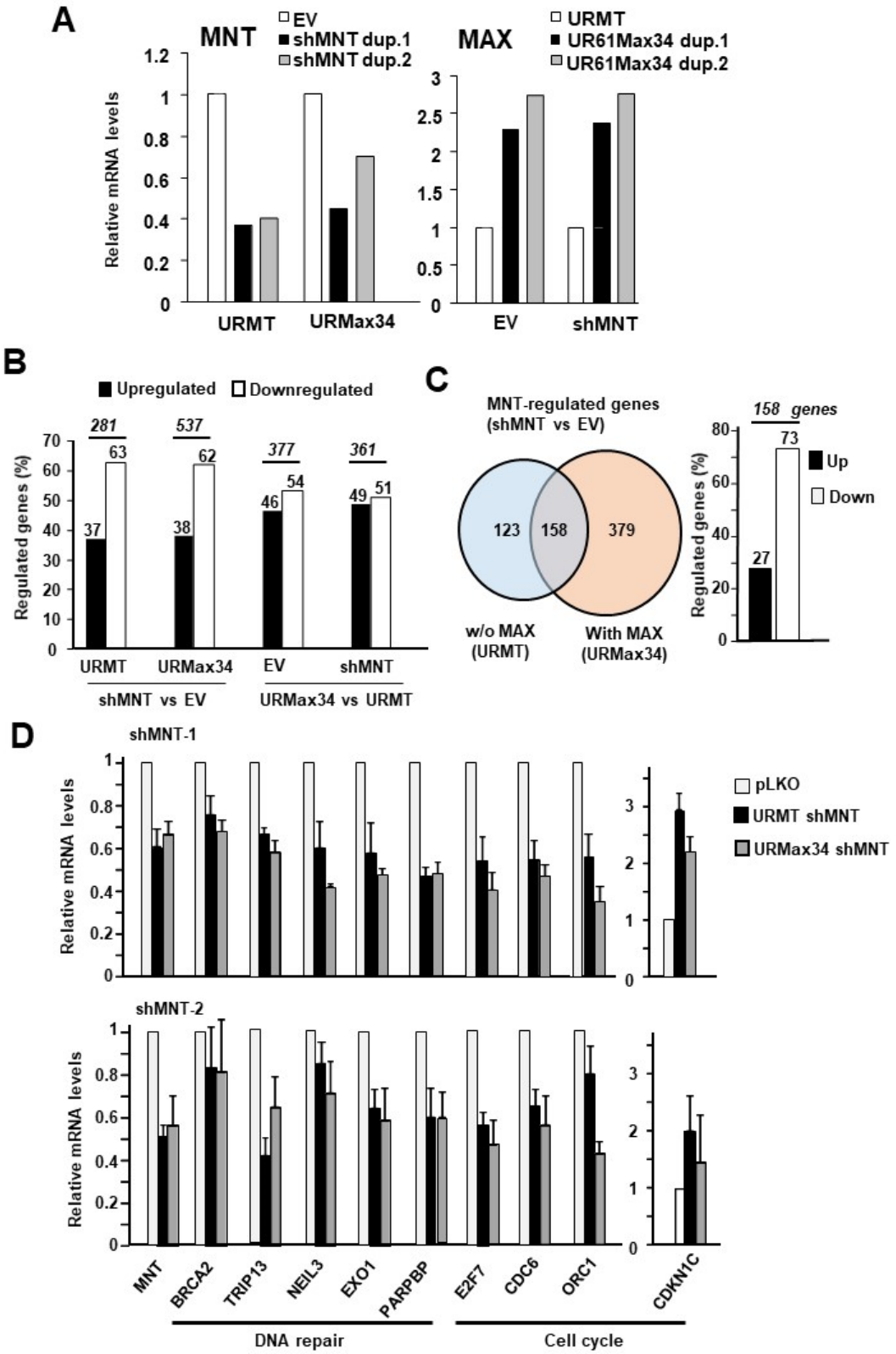

Figure 7. Gene expression changes in MNT knock-down cells. (A) mRNA expression of MNT and MAX in URMT and URMax34 cells lysed 72 h after transfection with sh-MNT and 24 h of treatment with 100 μM Zn^{2+}. The experiments were performed in duplicated (dup.1 and dup.2). These RNAs were subjected to RNA-seq. (B) Percentage of upregulated and downregulated genes in cells transfected with the shMNT or pLKO (empty) vectors URMT and URMax34 cells, as indicated at the bottom. The number of genes regulated comparing the different samples are indicated at the top of the figure. The gene inclusion criteria were a change in mRNA level ≥1.7 fold or ≤0.6 fold. The RNA-seq data are from two independent experiments. The genes regulated in the different comparisons are listed in the *Supplementary Tables 1 to 4*. (C) Venn diagram showing the genes that are regulated by MNT in MAX-deficient (URMT) or MAX-expressing cells (URMax34). The graph at the right shows the up- or down-regulated genes in the group of overlapping genes . (D) mRNA expression regulation due to MNT silencing in genes selected after the RNA-seq data. URMT and URMax34 were transfected with shMNT-1 (upper panel) and shMNT-2 (lower panel) or empty vector pLKO. After 48 h cells were treated for 24 h with 100 μM Zn^{2+}, total RNA was prepared and mRNA levels of the indicated genes were determined by RT-qPCR . Most of the selected genes are involved in DNA repair or cell cycle as indicated at the bottom. The data are represented as mean ±s.e.m. from four (shMNT-1) or three (shMNT-2) independent transfection experiments.

283 From the RNA-seq data we grouped, the genes that were up-regulated and
284 down-regulated in both duplicates considering a log2 RPKM fold change higher than 0.7
285 or smaller than -0.7 of the corresponding control. The heatmap of the gene expression
286 signature clearly shows that the depletion of MNT in both URMT and URMax34 induced
287 gene transcription changes (Supplementary Figure 3A,B) indicating that MNT is
288 important for the regulation of gene transcription. Specifically, 281 genes were regulated
289 upon MNT depletion in control URMT cells (Supplementary Table 1) and 537 genes in
290 MAX-expressing cells (i.e., URMax34 treated with Zn2+) (Supplementary Table 2).
291 Approximately 62 % of these genes were down-regulated upon MNT depletion (Figure
292 7B). In addition, URMax34 and URMT gene expression heatmaps clearly showed that
293 the expression of MAX induced gene transcriptional changes (Supplementary Figure
294 3C,D). When comparing URMax34 and URMT cells, 377 genes were found to be
295 differentially expressed (*Supplementary Table 3*). We also found 361 genes with
296 differential expression comparing URMax34 and URMT cells when both cell lines were
297 MNT-depleted and treated with Zn^{2+} (*Supplementary Table 4*). Among *MAX*-regulated
298 genes, roughly half of the genes were downregulated (*Figure 7B*).
299 The comparison between the lists of the genes regulated by MNT in cells without
300 MAX (URMT) and with MAX (URMax34) revealed 158 shared genes in the two
301 duplicates, meaning that 56% and 30% of the MNT-regulated genes in each cell line are
302 regulated by MNT in a MAX-independent manner (*Figure 7C*).
303 The genes showing expression changes in the MNT-depleted URMT and
304 URMax34 cells were analysed with the GSEA and the MsigDB platform
305 (http://software.broadinstitute.org/gsea/msigdb). The genes regulated upon MNT knock-
306 down were compared with the gene sets derived from the biological process gene
307 ontology and the comparison showed that genes belonging to cell cycle processes are
308 the most enriched set in MNT-depleted cells both in MAX expressing and not expressing
309 cells (*Supplementary Table 5*).
310 In order to explain the effects of MNT ablation on UR61 cell growth, we selected
311 several genes involved in cell cycle and DNA replication that were regulated in the RNA-
312 seq duplicates. URMT and URMax34 cells were transfeted with the two shMNT
313 constructs and the empty vector, and analysed the expression of these genes by RT-
314 qPCR. The *Figure 7D* shows that genes involved in cell cyle and DNA replication (*E2F7*,
315 *CDKN1C*, *CDC6*, *ORC1*) and DNA repair (*BRCA2*, *TRIP13*, *NEIL3*, *EXO1*, *PARPB*),
316 were down-regulated upon silencing of *MNT* with the two sh-MNT constructs, except
317 *CDKN1C* (p57, a cell cycle inhibitor) which was up-regulated. The results are consistent
318 with the negative effect of MNT depletion on cell proliferation (*Figure 6*).

319 We wondered how could MNT act as transcription factor in cells lacking MAX.
320 Besides MAX, MNT can also bind the HLH protein MLX *(Cairo et al 2001, Meroni et al*
321 *2000)*. To show if this interaction also takes place in UR61, we transfected MLX-Flag into
322 URMT cells and 48 h later lysates were immunoprecipitated MLX with anti-MLX antibody
323 and MNT with anti-MNT antibodies. The immunoprecipitates were analysed by

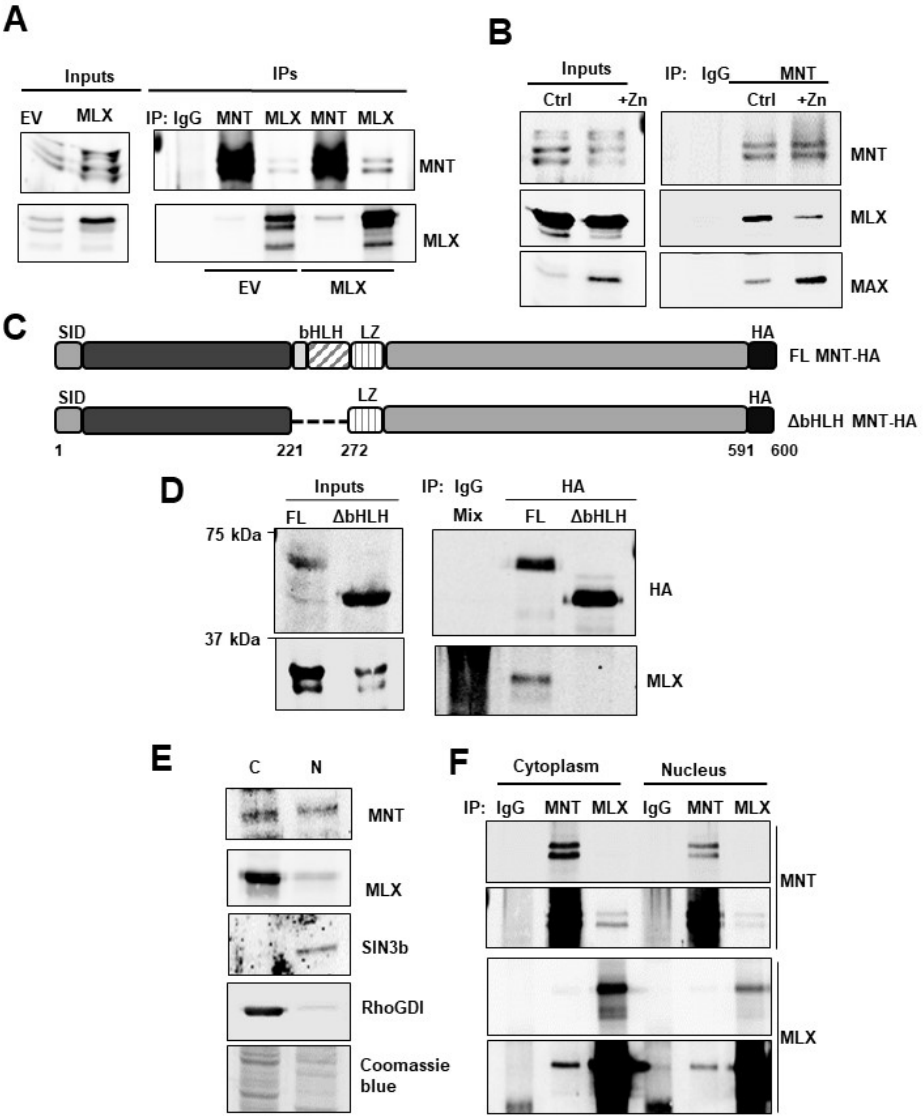

Figure 8. MNT and MLX interaction in UR61 cells.(A) URMT cells were transfected with a MLX expression vector or the empty vector (EV). 48 h after transfection, total cell lysates were prepared and precipitated with anti-MNT or anti-MLX antibodies, as well as unspecific IgG. The presence of MNT and MLX were detected in the immunoprecipitates by immunoblot. (B) URMax34 cells were transfected with a MLX expression vector and 48 h after transfection cells were treated with 100 μM Zn^{2+} for 24 h. Then total cell lysates were prepared and immunoprecipitated with anti-MNT. As a control, a mixture of lysates from cells treated and untreated with Zn^{2+} was immunoprecipitated with unspecific IgG. The presence of MNT, MLX and MAX in the immunoprecipitates were analysed by immunoblot. (C) Schematic representation of the full-length (FL) and the deletion mutant ΔHLH MNT-HA used in subsequent experiments. The SID (Sin3 Interacting Domain), bHLH, LZ domains, HA tag and amino acids of the murine protein are indicated. (D) URMT cells were co-transfected with a vector expressing MLX and the constructs shown in (C) as indicated at the top. 48 h after transfection, cell lysates were prepared and the cells were immunoprecipitated with mouse anti-HA antibody to pull down the exogenous MNT proteins constructs. As a control, lysates (a mixture of lysates from cell transfected with FL MNT and ΔHLH MNT) were also immunoprecipitated with unspecific IgGs. The immunoblot analysis using a rat monoclonal anti-HA antibody revealed the presence of FL MNT and the smaller ΔHLH MNT The presence of MLX in the immunoprecipitates was analysed with an anti-MLX antibody. (E) MLX localization in UR61 cells. Nuclear ("N") and cytoplasmic ("C") extracts were prepared from URMT cells as described in Materials and Methods and the levels of MNT and MLX were determined in each fraction by immunoblot. SIN3B and RhoGDI (ARHGDIA) were used as nuclear and cytoplasmic markers respectively. The antibodies used are as described in the *Supplementary Table 6.* A picture of the gel stained with Coomasie Blue after transference is also shown as an indicator of the total amount of proteins in the cytoplasmic and nuclear fraction. (F) Interaction between MNT and MLX in the nucleus and cytoplasm. URMT cells were transfected with a MLX expression vector and 48 h later nuclear and cytoplasmic extracts were prepared and immunoprecipitated with anti-MNT or anti-MLX antibodies. The levels of MNT and MLX in the immunoprecipitates were assayed by immunoblot.

324 immunoblot and the results showed the interaction between MNT and MLX (*Figure 8A*).
325 We next studied this interaction in URMax34 cells treated with Zn^{2+}, i.e. cells expressing
326 MAX. The immunoblot results showed that MNT and MLX also interacted but the
327 interaction was weaker when MAX expression was induced by Zn^{2+}. Thus, the data
328 suggest that, at least in our experimental conditions, MNT-MAX dimers were formed
329 more efficiently than MNT-MLX dimers (*Figure 8B*). To confirm the MNT-MLX interaction
330 in URMT cells, we prepared a HA-tagged MNT mutant with a deletion of most of the HLH
331 domain of mouse MNT, termed ΔHLHMNT-HA (*Figure 8C*). This mutant or the wild-type
332 counterpart was transfected into URMT and the corresponding lysates were
333 immunoprecipitated with anti-HA. The results showed that HLH domain is required for
334 the MNT-MLX interaction (*Figure 8D*).
335 In contrast to MAX, MLX is expressed in both nucleus and cytoplasm *(Billin et al*
336 *2000)*. By immunoblot analysis it was found that MLX was present in nucleus and, at a
337 lesser extent, in the cytoplasm of URMT cells (*Figure 8E*). Next, we prepared nuclear
338 and cytoplasmic fractions of URMT cells and studied by immunoprecipitation with anti-
339 MNT and anti-MLX antibodies if MNT and MLX interact. The results showed that this was
340 indeed the case in both nuclear and cytoplasmic fractions (*Figure 8F*). The proximity
341 ligation assay also showed that MNT and MLX interacted in both nucleus and cytoplasm
342 (not shown).
343 Finally, it is described that MNT can form homodimers in two-hybrid experiments
344 *(Hurlin et al 1997, Meroni et al 1997)*. Thus, a possibility is that MNT acts a transcription
345 factor as an homodimer. This homodimerization has not been demonstrated *in vivo* so
346 we tested it in HEK293T and UR61 cells. We first co-transfected HEK293T cells with
347 GFP-MNT and Flag-MNT constructs and immunoprecipitated with anti-GFP antibody.
348 The immunoblot analysis demonstrated the presence of the smaller Flag-MNT protein in
349 the material immunoprecipitated with anti-GFP (*Figure 9A*). As expected, both big and
350 small MNT forms were detected when the immunoblots were analysed with anti-MNT
351 antibody (*Figure 9A*). The results suggested the presence of homodimers between GFP-
352 MNT and MNT-Flag in HEK293T cells. As a control, the lysates with anti-MAX antibody
353 were immunoprecipitated, and both MNT and GFP-MNT were found to be bound to MAX
354 (not shown). Next, we investigated the MNT homodimerization in the UR61 system.
355 URMT cells were infected with lentiviral particles containing the GFP-MNT construct,
356 immunoprecipitated, and the lysates analysed by immunoblot with anti-GFP antibody
357 and anti-MNT antibodies. The results showed that MNT was present in the
358 immunoprecipitates with anti-GFP (*Figure 9B*). The results suggest that MNT forms
359 homodimers in human HEK293T cells and in MAX-deficient rat URMT cells. As MNT
360 dimerization in yeast two hybrid assays depends on the HLH-LZ *(Hurlin et al 1997,*

361 *Meroni et al 1997)*, we asked whether HLH was involved in the homodimerization *in vivo*.
362 We transfected the MNT mutant lacking the bHLH region (ΔbHLH MNT) (*Figure 8C*) as
363 well as the wild-type form and immunoprecipitated with anti-HA antibodies which should
364 only recognize the exogenous proteins. The immunoblot analysis of the
365 immunoprecipitates revealed that ΔbHLH MNT was unable to bind GFP-MNT (*Figure*
366 *9C*). The same experiment was performed in URMT cells and the same result was
367 observed, i.e, GFP-MNT bound to wild-type MNT-HA but not to the ΔbHLH form (*Figure*
368 *9D*). We conclude that bHLH domain is required for MNT homodimerization.

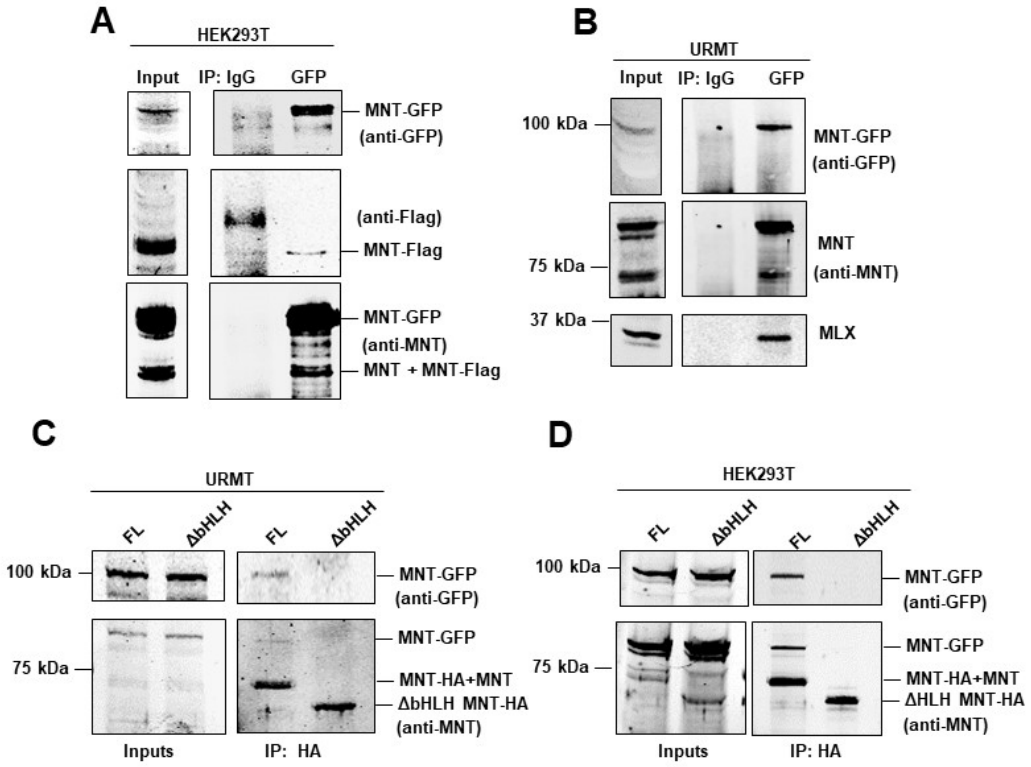

Figure 9. MNT homodimerization in UR61 cells. (A) HEK293T cells were co-transfected with a MNT-GFP and MNT-Flag expression vectors, and 24 h later lysates were prepared and immunoprecipitated with anti-GFP antibody. The presence of MNT-GFP and MNT-Flag were revealed by immunoblotting the antibodies indicated at the right. As a control, lysates were precipitated with unspecific IgG. The antibodies used in each immunoblot are indicated at the right. (B) URMT cells were infected with lentivirus encoding a MNT-GFP and 72 h later were transfected with MNT-Flag and treated with 15 nM bortezomib for 12 h before harvesting. 48 h after transfection lysates were prepared and immunoprecipitated with anti-GFP antibody. The presence of MNT-GFP, MNT and MLX in the immunoprecipitates were assessed by immunoblot. The antibodies used in each immunoblot are indicated at the right. (C) URMT cells were infected with lentivirus encoding a MNT-GFP and 72 h later transfected with expression vectors for FL MNT or ΔHLH MNT (Figure 8C) as indicated at the top of each lane. 48 h after transfection, cell lysates were prepared and immunoprecipitated with anti-HA to pull down the transfected MNT proteins. The levels of MNT-GFP and MNT were determined by immunoblot using anti-GFP and polyclonal anti-MNT antibody. (D) HEK293T cells were co-transfected with expression vectors for MNT-GFP and expression vectors for FL MNT or ΔHLH MNT (Figure 8C) as indicated at the top of each lane. 24 h later lysates were prepared and immunoprecipitated with anti-MNT antibody. The levels of MNT-GFP and MNT were determined by immunoblot using anti-GFP and polyclonal anti-MNT antibody.

371 **DISCUSSION**

372 In this study, we report five novel findings: (i) MNT is required for optimum proliferation
373 even in the absence of MAX; (ii) in the absence of MAX, MNT expression is elevated
374 and a significant fraction localizes in the cytoplasm; (iii) MNT represses its own
375 transcription in a MAX-dependent manner; (iv) MNT is able to regulate the expression of
376 genes in the absence of MAX and (v) MNT forms homodimers in vivo.. Previous reports

377 suggest that MNT functions as a “MYC buffer”, curbing excessive MYC activity whereas
378 MNT silencing leads to MYC-like phenotypes [reviewed in *(Diolaiti et al 2015, Yang &*
379 *Hurlin 2017)*]. Our data are in line with this critical MNT function, as they show a tight
380 control of MNT expression by which MNT limits its own mRNA expression. MNT protein
381 levels are also under strict control in UR61 cells, as MNT cannot be overexpressed at
382 high levels upon transfection unless the proteasome is inhibited. Given the relevance of
383 MNT to modulate MYC activity and its linking position between the MYC-MAX and MLX-
384 MONDO networks, the activities and regulation of MNT are a key issue on MYC-
385 dependent oncogenesis

386 MNT expression was high in MAX-deficient cells like the rat UR61 cells and
387 human lung carcinoma H1417 cells. The absence of MAX was in part responsible for this
388 effect because (i) MAX re-expression in UR61cells results in decreased MNT mRNA and
389 protein, and (ii) MAX overexpression in K562 cells results in MNT down-regulation
390 whereas MAX knock-down results in MNT up-regulation. The mechanism for this MAX
391 effect on MNT levels depended, at least partially, on the auto-repression of MNT
392 expression by MNT-MAX dimers. Luciferase reporter experiments showed that MNT
393 represses its own promoter (which contains two conserved E-boxes) and ChIP assays
394 showed that MNT binds to its own promoter when MAX is ectopically expressed in UR61
395 cells. In agreement with these results, significant levels of MNT localize to the cytoplasm
396 of MAX-deficient cells whereas MNT remains nuclear in MAX-expressing cells. This
397 would explain why MAX re-expression leads to a decrease in MNT levels: MNT-MAX
398 dimers would be formed to repress MNT expression in the nucleus. On the contrary, in
399 the absence of MAX, MNT is expressed at higher levels since there would be no negative
400 MNT autoregulation. The model is schematized in *Figure 10*.

401 We explored possible MAX-independent effects of MNT using the UR61 model.
402 Although originally MAX was defined as an obligate dimerization partner of MYC, work
403 carried out in the PC12 model and in *Drosophila* indicated that MYC can function in a
404 MAX-independent manner, for example in inhibition of differentiation *(Gallant 2013,*
405 *Maruyama et al 1987, Vaque et al 2008)*. MYC overexpression blocks RAS-induced
406 differentiation of UR61 cells *(Vaque et al 2008)* but we did not detect a significant effect
407 of MNT depletion on differentiation (not shown). In contrast, depletion of MNT in MAX-
408 deficient UR61 cells impairs cell proliferation. This is the first report on a MAX-
409 independent function of a MXD protein. In contrast, in rat and mouse fibroblasts, MNT
410 knock-out leads to increased proliferation and transformation capacities *(Hurlin et al*
411 *2003, Nilsson et al 2004)*. The fact that MNT depletion impairs UR61 proliferation (in a
412 MAX-independent manner) adds complexity in the MNT-MYC functional interactions.

Actually, in gastric cancer high MNT expression correlates with shorter survival whereas MYC overexpression has the opposite effect (http://kmplot.com/analysis/).

Since MNT is a transcription factor, we compared the transcriptomes of parental UR61 cells versus cells with depleted MNT. Upon MNT depletion, a number of genes involved in cell cycle progression and DNA damage response were downregulated in cells with and without MAX. This is concordant with the decrease in proliferation exerted by MNT silencing in UR61. It is open to discussion how MNT regulates genes in the absence of MAX. MNT can form heterodimers with the HLH protein MLX *(Cairo et al 2001, Meroni et al 2000)* and we have confirmed the ability of MNT to bind MLX in UR61 cells, although when MAX is expressed the dimers MNT-MAX re favoured versus MNT-MLX. As a relevant fraction of MLX is cytoplasmic and we have shown that MNT and MLX also interact in the cytoplasm, this interaction could help to explain the increase in cytoplasmic MNT in MAX-depleted cells. The model is depicted in the *Figure 10*. Moreover, we have shown that MNT homodimerizes in UR61 cells, and therefore it is likely that MNT regulates genes as an homodimer. Further work is required to clarify this point.

The results reported here show a strict autoregulation of MNT, supporting a pivotal role of MNT in the control of cell proliferation even in the absence of MAX. They also demonstrate that MNT has activities in the absence of MAX. Given that MNT participates in both the MAX-MYC and MLX-MONDO networks, the regulation of MNT is relevant in cell biology and in tumor development promoted by MYC.

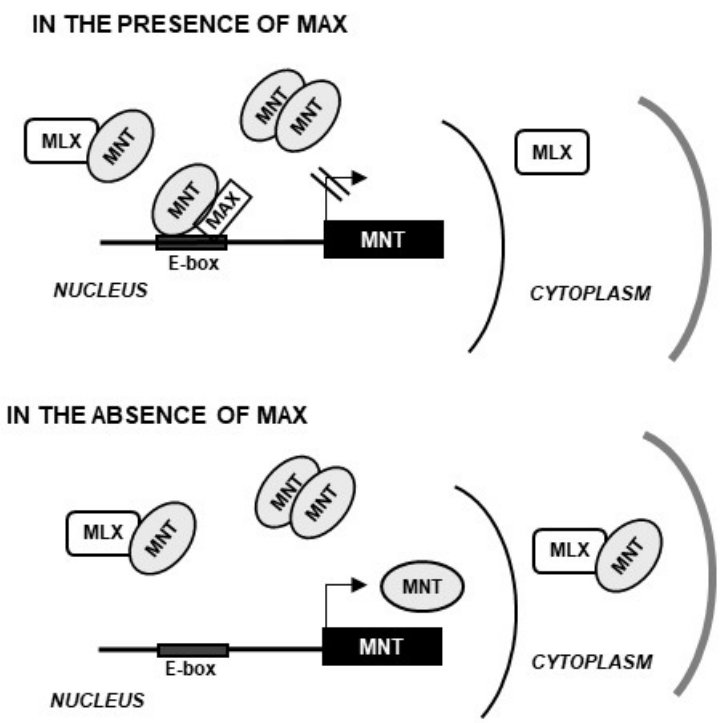

Figure 10. Model of MNT fates depending on MAX. In MAX-expressing cells, most of the MNT is retained in the cell nucleus where it limits its own expression. In MAX-deficient cells as UR61, MNT is distributed in nucleus and cytoplasm and is unable to bind the promoter and regulate its transcriptional activity. The model includes the presence of MNT-MNT homodimers and the interaction MNT-MLX in the cytoplasm, which might be responsible for the MNT partial localization in the cytoplasm in MAX-deficient cells

443 **MATERIALS AND METHODS**

444 ## Cell lines and transfections

445 Cell lines were obtained from ATCC and grown in either RPMI-1640 or DMEM (Lonza)
446 supplemented with 10% fetal bovine serum (Lonza), 150 µg/ml of gentamicin and 2 µg/ml
447 of ciprofloxacin. To generate the URMT and URMax34 cell line, UR61 cells *(Guerrero et*
448 *al 1988)* were electroporated (260 V, 1 mFa, BioRad apparatus) with a pHeBo-MT or
449 pHeBo-MT-Max vector which carries a human MAX cDNA under the control of
450 metallothionein promoter *(Canelles et al 1997)*. Cells were selected with 0.2 mg/ml of
451 hygromycin (Life Technologies) and cell clones were isolated by limiting dilution
452 Transient transfections were carried out using the Ingenio Electroporation solution
453 (Mirus) in an Amaxa nucleofector. The cells were transfected or transduced with
454 expression vectors for MAX (pCEFL-MAX*(Mauleon et al 2004)*, MLX (β isoform, (pMS18-
455 MLX,*(Billin et al 1999)*, human MNT (pCMVSport6-MNT, Origene Technologies), MNT-
456 Flag (human MNT with FLAG at the C-ter lentiviral Lv158 vector Genecopoeia), MNT-
457 GFP (human MNT with GFP at the N-ter, lentiviral Lv103 vector Genecopiea,), FL MNT-
458 HA (full-length murine MNT tagged at the C-ter with hemagglutinin epitope, HA), ΔHLH
459 MNT-HA (murine MNT carrying a deletion of amino acids 221-272 amino acids and
460 tagged with HA) (both in pcDNA3 with the zeocin resistance gene inserted), short-hairpin
461 human MNT-1 (shMNT-1, pLKO-shMNT from Sigma Mission, TRCN0000085733), or
462 MNT-2 (shMNT-2, pLKO-shMNT from Sigma Mission, TRCN0000235813), siRNA for
463 human MAX (Sigma, SASI_Hs01_00011941).
464

465 ## Immunoblot and immunoprecipitation

466 Cell lysis, immunoblots and immunoprecipitations were performed as described.*(Garcia-*
467 *Sanz et al 2014)* .The antibodies used are described in *Supplementary Table 6.*

468 ## Luciferase reporters and assays

469 To generate the 850MNT-luc, 220MNT-luc, 570MNT-luc reporter vectors, two pair of
470 primers were designed for each construct (*Supplementary Table 7*), targeting sequences
471 of the human genome corresponding to 850 bp upstream the transcription start site
472 (TSS) of *MNT* gene. The amplified DNA was inserted into the pBV-luc reporter vector at
473 the EcoRV and HindIII sites *(He et al 1998)*. The sequence of MNT promoter was from
474 the UCSC genome browser (http://genome.ucsc.edu/; GRCh37/hg19). Cells were
475 transfected with jetPEI reagent (Polyplus) and luciferase assays were performed as
476 described *(Garcia-Sanz et al 2014)*.
477

478 **Cell proliferation and cell cycle analysis**

479 Cell proliferation was monitored with a cell counter (NucleoCounter NC-100,
480 Chemometec) or a cytometer (Guava PCA, Merck Millipore). For the clonogenic assays,
481 1-2 x 10^6 cells/ml were seeded in a 6-well or 60 mm plate after transfection by
482 electroporation. 48 h post-transfection, cells were selected with puromycin at 0.2-0.5
483 µg/ml final concentration. After 8-17 days the cells were stained with crystal violet and
484 the dye measured by absorbance at 595 nm as described *(Ferrandiz et al 2009)*. To
485 determine the sugG0-G1 population, cells were transfected and 7 days post-transfection
486 the DNA concentration was analyzed by propidium iodide staining and flow cytometry
487 as described *(Albajar et al 2011)*.

488

489 **RNA analysis**

490 For qPCR, total RNA was isolated using the TRI Reagent® Solution (Invitrogen). cDNA
491 was generated by reverse transcription (RT) using the iScript (Bio-Rad). Quantitative
492 polymerase chain reaction (qPCR) was performed with specific primers (*Supplementary*
493 *Table 7*) using the iTaq™ Universal SYBR® Green Supermix (Bio-Rad) and CFX
494 ConnectTM Real-Time PCR Detection System (Bio-Rad). RNA was converted into cDNA
495 and analysed as described *(Bretones et al 2011)*. Levels of mRNA were normalized
496 against actin and RPS14 mRNA levels. For RNA-seq, total RNA was isolated with the
497 RNeasy kit (Qiagen) from two independent experiments of MNT silencing in URMT and
498 URMax34 cells, both treated with 100 µM $ZnSO_4$ for 24 h. mRNA libraries were prepared
499 using the Illumina TruSeq RNA Sample Prep Kit v2 (kit RS-122-2002, Illumina). A
500 minimum of 40 million 50 bases single-end reads per sample were obtained. Tophat
501 algorithm *(Trapnell et al 2009)* was used to align the data using a set of gene model
502 annotations and/or known transcripts of rat genome (rn4) obtained from RefSeq
503 database. Cufflinks software *(Trapnell et al 2010)* was run to estimate transcripts
504 abundances represented in RPKM units (reads per kilobase per million reads) as
505 described (Mortazavi et al 2008). The gene expression of the genes included in
506 *Supplementary Tables* 1-4 are represented as RPKM values and the threshold for
507 expression changes was set as log2(RPKM fold change) ≥ 0.7 or ≤ -0.7 and a p-value
508 <0.1.

509

510 **Bioinformatic analysis**

511 Genomic sequences of 1000 bp upstream TSS of human, mouse and rat MNT genes
512 were obtained from *H. sapiens* (GRCh37/hg19), *M. musculus* (GRCm38/mm10) and *R.*
513 *norvegicus* (RGSC 5.0/rn5) assemblies. For the ChIP-seq ENCODE analysis, the data

514 for MAX, MYC and MXI1 was obtained for the indicated cell lines. The SYDH ENCODE
515 project was chosen for representation of the binding peaks in the promoter of the human
516 MNT gene. The sequences corresponding to those peaks were analysed confirming the
517 presence of the E-boxes identified in the human MNT promoter.
518

519 **Chromatin immunoprecipitation**

520 Fractionation of total cell extracts into cytoplasmic and nuclear fractions and chromatin
521 immunoprecipitation (ChIP) were performed essentially as described *(Garcia-Sanz et al*
522 *2014)*. Immunoprecipitated DNA was purified with the QIAquick PCR Purification
523 Kit (Qiagen) and analysed by qPCR. The antibodies and primers used are described in
524 *Supplementary Tables 6 and 7*, respectively.
525

526 **Nuclear/cytoplasmic fractionation**

527 Cytoplasmic and nuclear extracts were prepared essentially as described *(Conacci-*
528 *Sorrell et al 2010)*. The hypotonic buffer to lyse cells was 10 mM HEPES pH 7, 10 mM
529 KCl, 0.25 mM EDTA pH 8, 0.125 mM EGTA pH 8, 0.5 mM spermidin, 0.1% NP40, 1 mM
530 DTT and proteases inhibitors The hypertonic buffer for nuclear extracts was 20 mM
531 HEPES, 400 mM NaCl, 0.25 mM EDTA, 1.5 mM $MgCl_2$, 0.5 mM DTT and proteases
532 inhibitors.
533

534 **ACKNOWLEDGEMENTS**

535 The work was supported by grant SAF2014-53526-R from MINECO, Spanish
536 Government, to JL and MDD (partially funded by FEDER program from European Union)
537 RNE is supported by grant CA57138/CA/NCI from National Institutes of Health. PJH is
538 supported by grants from Shriners Hospitals for Children. MCL-N and JL-P were
539 recipients of F.P.U. fellowships from Spanish Government. We are grateful to Montserrat
540 Sánchez-Céspedes and Don Ayer for reagents, and Sandra Zunzunegui and Maria
541 Aramburu for technical help.
542

543 **CONFLICT OF INTEREST**

544 The authors declare no conflict of interests
545
546

547 **REFERENCES**

548 Albajar M, Gomez-Casares MT, Llorca J, Mauleon I, Vaque JP, Acosta JC, Bermudez
549 A, Donato N, Delgado MD, Leon J. 2011. MYC in chronic myeloid leukemia:
550 induction of aberrant DNA synthesis and association with poor response to
551 imatinib. Mol Cancer Res 9: 564-76
552 Billin AN, Eilers AL, Coulter KL, Logan JS, Ayer DE. 2000. MondoA, a novel basic
553 helix-loop-helix-leucine zipper transcriptional activator that constitutes a positive
554 branch of a max-like network. Mol Cell Biol 20: 8845-54
555 Billin AN, Eilers AL, Queva C, Ayer DE. 1999. Mlx, a novel Max-like BHLHZip protein
556 that interacts with the Max network of transcription factors. J Biol Chem 274:
557 36344-50
558 Bretones G, Acosta JC, Caraballo JM, Ferrandiz N, Gomez-Casares MT, Albajar M,
559 Blanco R, Ruiz P, Hung WC, Albero MP, Perez-Roger I, Leon J. 2011. SKP2
560 oncogene is a direct MYC target gene and MYC down-regulates p27(KIP1)
561 through SKP2 in human leukemia cells. J Biol Chem 286: 9815-25
562 Cairo S, Merla G, Urbinati F, Ballabio A, Reymond A. 2001. WBSCR14, a gene
563 mapping to the Williams--Beuren syndrome deleted region, is a new member of
564 the Mlx transcription factor network. Hum Mol Genet 10: 617-27
565 Canelles M, Delgado MD, Hyland KM, Lerga A, Richard C, Dang CV, Leon J. 1997.
566 Max and inhibitory c-Myc mutants induce erythroid differentiation and resistance
567 to apoptosis in human myeloid leukemia cells. Oncogene 14: 1315-27
568 Conacci-Sorrell M, McFerrin L, Eisenman RN. 2014. An Overview of MYC and Its
569 Interactome. Cold Spring Harb Perspect Med 4: 1-24
570 Conacci-Sorrell M, Ngouenet C, Eisenman RN. 2010. Myc-nick: a cytoplasmic
571 cleavage product of Myc that promotes alpha-tubulin acetylation and cell
572 differentiation. Cell 142: 480-93
573 Dang CV. 2012. MYC on the path to cancer. Cell 149: 22-35
574 Dezfouli S, Bakke A, Huang J, Wynshaw-Boris A, Hurlin PJ. 2006. Inflammatory
575 disease and lymphomagenesis caused by deletion of the Myc antagonist Mnt in
576 T cells. Mol Cell Biol 26: 2080-92
577 Diolaiti D, McFerrin L, Carroll PA, Eisenman RN. 2015. Functional interactions among
578 members of the MAX and MLX transcriptional network during oncogenesis.
579 Biochim Biophys Acta 1849: 484-500
580 Ferrandiz N, Martin-Perez J, Blanco R, Donertas D, Weber A, Eilers M, Dotto P,
581 Delgado MD, Leon J. 2009. HCT116 cells deficient in p21(Waf1) are
582 hypersensitive to tyrosine kinase inhibitors and adriamycin through a
583 mechanism unrelated to p21 and dependent on p53. DNA Repair 8: 390-9
584 Foley KP, McArthur GA, Queva C, Hurlin PJ, Soriano P, Eisenman RN. 1998. Targeted
585 disruption of the MYC antagonist MAD1 inhibits cell cycle exit during
586 granulocyte differentiation. EMBO J 17: 774-85
587 Gallant P. 2013. Myc function in Drosophila. Cold Spring Harb Perspect Med 3:
588 a014324
589 Garcia-Sanz P, Quintanilla A, Lafita MC, Moreno-Bueno G, Garcia-Gutierrez L, Tabor
590 V, Varela I, Shiio Y, Larsson LG, Portillo F, Leon J. 2014. Sin3b interacts with
591 myc and decreases myc levels. J Biol Chem 289: 22221-36
592 Guerrero I, Pellicer A, Burstein DE. 1988. Dissociation of c-fos from ODC expression
593 and neuronal differentiation in a PC12 subline stably transfected with an
594 inducible N-ras oncogene. Biochem Biophys Res Commun 150: 1185-92
595 He TC, Sparks AB, Rago C, Hermeking H, Zawel L, da Costa LT, Morin PJ, Vogelstein
596 B, Kinzler KW. 1998. Identification of c-MYC as a target of the APC pathway.
597 Science 281: 1509-12
598 Hopewell R, Ziff EB. 1995. The nerve growth factor-responsive PC12 cell line does not
599 express the Myc dimerization partner Max. Mol Cell Biol 15: 3470-8

600 Hurlin PJ, Queva C, Eisenman RN. 1997. Mnt, a novel Max-interacting protein is
601 coexpressed with Myc in proliferating cells and mediates repression at Myc
602 binding sites. Genes Dev 11: 44-58.
603 Hurlin PJ, Zhou ZQ, Toyo-oka K, Ota S, Walker WL, Hirotsune S, Wynshaw-Boris A.
604 2003. Deletion of Mnt leads to disrupted cell cycle control and tumorigenesis.
605 EMBO J 22: 4584-96
606 Lafita-Navarro MC, Blanco R, Mata-Garrido J, Liano-Pons J, Tapia O, Garcia-Gutierrez
607 L, Garcia-Alegria E, Berciano MT, Lafarga M, Leon J. 2016. MXD1 localizes in
608 the nucleolus, binds UBF and impairs rRNA synthesis. Oncotarget 7: 69536-48
609 Link JM, Ota S, Zhou ZQ, Daniel CJ, Sears RC, Hurlin PJ. 2012. A critical role for Mnt
610 in Myc-driven T-cell proliferation and oncogenesis. Proc Natl Acad Sci U S A
611 109: 19685-90
612 Maruyama K, Schiavi SC, Huse W, Johnson GL, Ruley HE. 1987. myc and E1A
613 oncogenes alter the responses of PC12 cells to nerve growth factor and block
614 differentiation. Oncogene 1: 361-7
615 Mauleon I, Lombard MN, Munoz-Alonso MJ, Canelles M, Leon J. 2004. Kinetics of
616 myc-max-mad gene expression during hepatocyte proliferation in vivo:
617 Differential regulation of mad family and stress-mediated induction of c-myc.
618 Mol Carcinog 39: 85-90
619 Meroni G, Cairo S, Merla G, Messali S, Brent R, Ballabio A, Reymond A. 2000. Mlx, a
620 new Max-like bHLHZip family member: the center stage of a novel transcription
621 factors regulatory pathway? Oncogene 19: 3266-77
622 Meroni G, Reymond A, Alcalay M, Borsani G, Tanigami A, Tonlorenzi R, Nigro CL,
623 Messali S, Zollo M, Ledbetter DH, Brent R, Ballabio A, Carrozzo R. 1997. Rox,
624 a novel bHLHZip protein expressed in quiescent cells that heterodimerizes with
625 Max, binds a non-canonical E box and acts as a transcriptional repressor.
626 EMBO J 16: 2892-906.
627 Mortazavi A, Williams BA, McCue K, Schaeffer L, Wold B. 2008. Mapping and
628 quantifying mammalian transcriptomes by RNA-Seq. Nat Methods 5: 621-8
629 Nilsson JA, Maclean KH, Keller UB, Pendeville H, Baudino TA, Cleveland JL. 2004.
630 Mnt loss triggers Myc transcription targets, proliferation, apoptosis, and
631 transformation. Mol Cell Biol 24: 1560-9
632 Popov N, Wahlstrom T, Hurlin PJ, Henriksson M. 2005. Mnt transcriptional repressor is
633 functionally regulated during cell cycle progression. Oncogene 24: 8326-37
634 Queva C, McArthur GA, Ramos LS, Eisenman RN. 1999. Dwarfism and dysregulated
635 proliferation in mice overexpressing the MYC antagonist MAD1. Cell Growth
636 Differ 10: 785-96
637 Romero OA, Torres-Diz M, Pros E, Savola S, Gomez A, Moran S, Saez C, Iwakawa R,
638 Villanueva A, Montuenga LM, Kohno T, Yokota J, Sanchez-Cespedes M. 2014.
639 MAX inactivation in small cell lung cancer disrupts MYC-SWI/SNF programs
640 and is synthetic lethal with BRG1. Cancer Discov 4: 292-303
641 Schreiber-Agus N, DePinho RA. 1998. Repression by the Mad(Mxi1)-Sin3 complex.
642 Bioessays 20: 808-18
643 Terragni J, Nayak G, Banerjee S, Medrano JL, Graham JR, Brennan JF, Sepulveda S,
644 Cooper GM. 2011. The E-box binding factors Max/Mnt, MITF, and USF1 act
645 coordinately with FoxO to regulate expression of proapoptotic and cell cycle
646 control genes by phosphatidylinositol 3-kinase/Akt/glycogen synthase kinase 3
647 signaling. J Biol Chem 286: 36215-27
648 Toyo-oka K, Hirotsune S, Gambello MJ, Zhou ZQ, Olson L, Rosenfeld MG, Eisenman
649 R, Hurlin P, Wynshaw-Boris A. 2004. Loss of the Max-interacting protein Mnt in
650 mice results in decreased viability, defective embryonic growth and craniofacial
651 defects: relevance to Miller-Dieker syndrome. Hum Mol Genet 13: 1057-67
652 Trapnell C, Pachter L, Salzberg SL. 2009. TopHat: discovering splice junctions with
653 RNA-Seq. Bioinformatics 25: 1105-11

654 Trapnell C, Williams BA, Pertea G, Mortazavi A, Kwan G, van Baren MJ, Salzberg SL,
655 Wold BJ, Pachter L. 2010. Transcript assembly and quantification by RNA-Seq
656 reveals unannotated transcripts and isoform switching during cell differentiation.
657 Nat Biotechnol 28: 511-5
658 Vaque JP, Fernandez-Garcia B, Garcia-Sanz P, Ferrandiz N, Bretones G, Calvo F,
659 Crespo P, Marin MC, Leon J. 2008. c-Myc inhibits Ras-mediated differentiation
660 of pheochromocytoma cells by blocking c-Jun up-regulation. Mol Cancer Res 6:
661 325-39
662 Walker W, Zhou ZQ, Ota S, Wynshaw-Boris A, Hurlin PJ. 2005. Mnt-Max to Myc-Max
663 complex switching regulates cell cycle entry. J Cell Biol 169: 405-13
664 Yang G, Hurlin PJ. 2017. MNT and Emerging Concepts of MNT-MYC Antagonism.
665 Genes 8: pii: E83

666